Steady-state susceptibility in continuous phase transitions of dissipative systems

Xingli Li, Yan Li, and Jiasen Jin *
School of Physics, Dalian University of Technology, 116024 Dalian, China

(Received 12 January 2022; revised 9 April 2022; accepted 17 May 2022; published 27 May 2022)

In this work we explore the critical behaviors of fidelity susceptibility and trace distance susceptibility associated with the steady states of dissipative systems at continuous phase transitions. We investigate two typical models: One is the dissipative spin-$1/2$ XYZ model on a two-dimensional square lattice and the other is a driven-dissipative Kerr oscillator. We find that the susceptibilities of fidelity and trace distance exhibit singular behaviors near the critical points of phase transitions in both models. The critical points in the thermodynamic limit, extracted from the scalings of the critical controlling parameters to the system size or nonlinearity, agree well with the existing results.

DOI: 10.1103/PhysRevA.105.052226

I. INTRODUCTION

Phase transition is the key concept in condensed matter and statistical physics [1]. In general, quantum phase transitions in the equilibrium case always signify that the ground-state properties of the quantum many-body systems have changed. In particular, the correlation length, magnetic susceptibility, entanglement, and other physical quantities exhibit divergent behaviors at the critical point [2]. However, a realistic system is always regarded as an open system due to the inevitable interactions with its environment [3–5]. The dissipation induced by the system-environment interactions drives the open system away from equilibrium. The phase transition may also occur in open quantum many-body systems manifested by the emergence of an ordered steady state in the long-time limit when tuning the controllable parameter [6,7]. Investigating such nonequilibrium phase transitions is of great significance not only in the understanding of the collective phenomena and dynamics of dissipative systems, but also in highlighting the possibilities of quantum information processing in open systems, such as quantum state engineering and quantum sensing.

Due to the nonunitary nature of the dynamics and exponential growth of the dimension of Hilbert space of the system, its theoretical description and numerical simulation for open quantum many-body systems are challenging. In recent years, plenty of meaningful results have been obtained [8–14] and several numerical methods have been developed [15–24]. By combining the corner-space renormalization method [19] with the Monte Carlo wave-function trajectory method [25], Rota *et al.* investigated the divergence of the angularly averaged magnetic susceptibility in the two-dimensional dissipative spin-$1/2$ XYZ model on a square lattice. With the finite-size scaling analysis, they obtained the critical point of the phase transition from paramagnetic to ferromagnetic phases. The corresponding critical exponents are obtained as well. Besides the angularly averaged magnetic susceptibility and von Neumann entropy, they found that the multipartite entanglement witnessed by the quantum Fisher information also exhibits the critical behavior when the controlling parameter is close to the critical point [26]. An alternative way to uncover the dissipative phase transition is to investigate the system through the dynamical behavior which is related to the Liouvillian spectrum. The Liouvillian gap tends to close when the system approaches the critical point; as a consequence, the system takes a longer time to reach the steady state. The critical slowing down has been observed in the two-dimensional driven-dissipative Bose-Hubbard model [27] and the dissipative spin-$1/2$ XYZ model [28]. Meanwhile, for the latter model, the Liouvillian gap saturates for the one-dimensional case, signaling the absence of the dissipative phase transition.

Different from the previous studies on the dissipative quantum many-body system, in this work we mainly focus on an observable-independent way to estimate the critical point, which is derived from the response degree of the steady states of the system to the parameter perturbations. To be more precise, we determine the critical point by intuitively giving the degree of similarity of the steady states of the system before and after the perturbation. The basic idea is that, in the thermodynamic limit, when the dissipative systems undergo the phase transitions by tuning the controlling parameter of the Hamiltonian, not only do the steady-state order parameters that belong to different phases change abruptly, but also the similarity between the two steady states shows a significant dip in the vicinity of the phase transition, e.g., the fidelity may exhibit divergent behavior in phase transitions of the closed system [29,30]. However, because the dimension of the Hilbert space in a practical simulation is limited by the computational power, the singular behavior of the similarity of steady states in different phases is usually not revealed. Here we utilize the fidelity susceptibility χ_F as an indicator to reveal the singular behavior.

The fidelity susceptibility, which is a higher-order derivative of fidelity, originates from the linear response theory and differential-geometric approach [31]. It is sensitive in reflecting the stability of a given system to the parameter

*jsjin@dlut.edu.cn

perturbation. Actually, the fidelity susceptibility has already been widely used in characterizing the ground-state phase transition in equilibrium. The nonanalytic divergence behavior of the fidelity susceptibility has been observed in the phase transitions of first and second orders [32–36]. Moreover, the fidelity susceptibility has also been used to investigate nonzero temperature phase transitions [37] and topological phase transitions [38,39].

In this paper, inspired by the good performance of fidelity susceptibility in characterizing the equilibrium phase transitions, we employ the fidelity susceptibility χ_F and trace distance susceptibility χ_T to investigate the dissipative phase transitions in open quantum many-body systems. We determine the critical points by finite-size scaling analysis on both χ_F and χ_T for the dissipative spin-1/2 XYZ model on a two-dimensional square lattice on which the existence of a steady-state phase transition from the normal paramagnetic to the ordered ferromagnetic phases has been verified by many numeric methods. Our results show that both quantities, which are observable independent, exhibit nonanalytic singular behaviors in the vicinity of the phase transitions. We also investigate the system of a driven-dissipative Kerr oscillator. We verify the existence of the continuous steady-state phase transition through the semiclassical approximation and obtain similar results near the phase transition.

This paper is organized as follows. In Sec. II we introduce the theoretical framework of the fidelity susceptibility and the trace distance susceptibility for mixed states. In Sec. III A we investigate the critical behavior of the two-dimensional spin-1/2 XYZ model on a square lattice and determine the critical exponents. In Sec. III B we employ the semiclassical approximation as a preliminary exploration and then identify the occurrence of dissipative phase transitions in the driven-dissipative Kerr oscillator model. We summarize in Sec. IV.

II. THEORETICAL FRAMEWORK

In this section we introduce the theoretic description of the dynamics of open quantum many-body systems and the concepts of fidelity susceptibility and trace distance susceptibility. We focus on the quantum many-body systems that are subjected to local environments. Under the Markovian approximation, the dynamics of the system's density matrix can be described by the Lindblad master equation ($\hbar = 1$ hereinafter)

$$\frac{\partial \hat{\rho}}{\partial t} = \mathcal{L}\hat{\rho}(t) = -i[\hat{H}, \hat{\rho}] + \sum_j \mathcal{D}_j[\hat{\rho}], \tag{1}$$

where $\mathcal{L}$ is the non-Hermitian Liouvillian superoperator, $\hat{H}$ is the Hamiltonian of the many-body system, and the dissipator $\mathcal{D}_j[\hat{\rho}]$ rules the interplay between the system and the local external environment. The first term on the right-hand side of Eq. (1) describes the coherent time evolution ruled by the Hamiltonian, while the second term describes the incoherent dissipation due to the system-environment interaction.

In general, the eigenspectrum of the superoperator $\mathcal{L}$ is complex. The eigenvalue equation is given by

$$\mathcal{L}\hat{\rho}_i = \lambda_i \hat{\rho}_i, \tag{2}$$

where λ_i $(i = 0, 1, 2, \ldots)$ and $\hat{\rho}_i$ are the eigenvalues and (normalized) eigenstates of $\mathcal{L}$, respectively. Usually the eigenvalues are sorted by the real parts as $\mathrm{Re}[\lambda_0] > \mathrm{Re}[\lambda_1] > \mathrm{Re}[\lambda_2] > \cdots$. The real parts of the eigenvalues are negative semidefinite. There is always at least one zero eigenvalue and the associated eigenstate is considered to be the steady state, which is defined as $\hat{\rho}_{\mathrm{SS}} = \hat{\rho}_0$ (the subscript SS denotes steady state). This can be understood as follows. Suppose that the system is initialized in the state $\hat{\rho}(0) = \sum_i c_i \hat{\rho}_i$, where c_i are the probability amplitudes. According to Eq. (2), the state of the system at arbitrary time evolves to $\hat{\rho}(t) = \sum_i e^{\lambda_i t} c_i \rho_i$. Apparently, after a sufficiently long time, all the eigenstates disappear asymptotically except for $\hat{\rho}_0$. Moreover, the eigenvalue with the largest nonzero real part is defined as the Liouvillian gap or the asymptotic decay rate [40]. The associated eigenstate decays slowest. By tuning the controllable parameter p in the Hamiltonian, the Liouvillian gap may start to close at a critical point p_c, indicating the occurrence of the continuous steady-state phase transition in open quantum many-body systems [41].

The steady-state phases are characterized by the order parameter $\langle\hat{O}\rangle_{\mathrm{SS}} = \mathrm{Tr}(\hat{\rho}_{\mathrm{SS}}\hat{O})$, which is the expected value of an appropriate observable $\hat{O}$ in the steady state. The nonzero order parameter indicates the ordered steady-state phase. In particular, the Mth-order phase transition can be defined as [41]

$$\lim_{p\to p_c} \left| \frac{\partial^M}{\partial p^M} \langle\hat{O}\rangle_{\mathrm{SS}} \right| \to +\infty. \tag{3}$$

The discontinuity of the Mth-order derivatives of the order parameter implies that the properties of the steady states are dramatically changed. It should be noted that the observable $\hat{O}$ is parameter p independent, which means that the singularity in Eq. (3) stems from the steady-state density matrix itself. This reminds us that the abrupt change of the similarity between the states associated with two close parameters may signal the occurrence of phase transition.

In the thermodynamic limit, if the Hamiltonian at the critical point is perturbed to $\hat{H}(p_c) \to \hat{H}(p_c + \delta p)$, the perturbed Hamiltonian can be expressed as

$$\hat{H}(p_c + \delta p) = \hat{H}(p_c) + \hat{H}(\delta p). \tag{4}$$

The corresponding steady states are denoted by $\hat{\rho}_{\mathrm{SS}}(p_c)$ and $\hat{\rho}_{\mathrm{SS}}(p_c + \delta p)$, respectively. When the parameter perturbation drives the system across the critical point, the properties of the steady states belonging to different phases will change remarkably. Along this line, quantifying the differences between two steady states in different phases may help us determine the critical point.

The fidelity quantifies the overlap between two given quantum states. It was introduced to characterize the response of a quantum system to a perturbation [42]. The fidelity is a non-negative, continuous, and symmetric function and it is invariant under unitary transformation [43]. The fidelity between the steady states associated with $\hat{H}(p)$ and $\hat{H}(p + \delta p)$ in the Hamiltonian is given by Uhlmann as follows [31,44]:

$$F(p, p + \delta p) = \mathrm{Tr}\sqrt{\sqrt{\hat{\rho}_{\mathrm{SS}}(p)}\hat{\rho}_{\mathrm{SS}}(p + \delta p)\sqrt{\hat{\rho}_{\mathrm{SS}}(p)}}. \tag{5}$$

For sufficiently small perturbation, one can expand Eq. (5) in powers of δp,

$$F(p, p+\delta p)_{\delta p\to 0} \simeq 1 - \frac{\chi_F(p, p+\delta p)}{2}\delta p^2 + \cdots + O(\delta p^n). \tag{6}$$

The fidelity susceptibility is defined by the coefficient of the quadratic term χ_F, which characterizes the response of fidelity to the parameter p. The definition of χ_F is rooted in the Bures distance between two infinitesimally close density matrices [45]; the expression is governed by [46]

$$\chi_F(p, p+dp) = \frac{1}{2}\sum_{n,m}\frac{|\langle m|\delta\hat{\rho}|n\rangle|^2}{\lambda_m+\lambda_n}, \tag{7}$$

where $\delta\hat{\rho} = \hat{\rho}_{\rm SS}(p+\delta p) - \hat{\rho}_{\rm SS}(p)$ and $|n\rangle$ is the eigenstate associated with the eigenvalue λ_n of the steady state $\hat{\rho}_{\rm SS}(p)$. In brief, the fidelity susceptibility is the higher-order derivative of the fidelity, which means this quantity is much more sensitive to perturbation.

There are also alternative quantities that can be used to measure the difference between two density matrices. For example, the trace distance measures the distance of two quantum states in Hilbert space, which satisfies the non-negative definiteness, the homogeneity, and the triangle inequality [47]. Hence, different from the quantum fidelity, the trace distance is a real distance in Hilbert space. For two arbitrary steady states $\hat{\rho}_{\rm SS}(p_A)$ and $\hat{\rho}_{\rm SS}(p_B)$, the trace distance was originally defined as

$$\begin{aligned} &T(p_A, p_B)\\ &:= \tfrac{1}{2}\|\hat{\rho}_{\rm SS}(p_B) - \hat{\rho}_{\rm SS}(p_A)\|_1\\ &= \tfrac{1}{2}\mathrm{Tr}\{\sqrt{[\hat{\rho}_{\rm SS}(p_B) - \hat{\rho}_{\rm SS}(p_A)]^\dagger[\hat{\rho}_{\rm SS}(p_B) - \hat{\rho}_{\rm SS}(p_A)]}\}. \end{aligned} \tag{8}$$

Consider two steady states as $\hat{\rho}_{\rm SS}(p_A) = \hat{\rho}_{\rm SS}(p)$ and $\hat{\rho}_{\rm SS}(p_B) = \hat{\rho}_{\rm SS}(p+\delta p)$, with δp the parameter perturbation. We obtain a more refined form of the trace distance

$$T(p_A, p_B) = \tfrac{1}{2}\mathrm{Tr}(\sqrt{\delta\hat{\rho}^\dagger\delta\hat{\rho}}), \tag{9}$$

where $\delta p = \hat{\rho}_{\rm SS}(p+\delta p) - \hat{\rho}_{\rm SS}(p)$. Now we can define the trace distance susceptibility as

$$\chi_T(p+\delta p, p) = \tfrac{1}{2}\mathrm{Tr}(\sqrt{\delta\hat{\rho}^\dagger\delta\hat{\rho}})/\delta p. \tag{10}$$

III. RESULTS

In this section we investigate both the fidelity susceptibility and trace distance susceptibility in two specific models. We analyze their scaling behaviors when the controllable parameters go across the steady-state phase transitions to extract the information of the critical points.

A. Dissipative spin-1/2 XYZ model

We start with the model of spin-1/2 particles on the square lattice in two dimensions. The Hamiltonian of the many-body system is given by the anisotropic Heisenberg interactions as

$$\hat{H} = \sum_{\langle j,l\rangle} J_x\hat{\sigma}_j^x\hat{\sigma}_l^x + J_y\hat{\sigma}_j^y\hat{\sigma}_l^y + J_z\hat{\sigma}_j^z\hat{\sigma}_l^z, \tag{11}$$

where $\hat{\sigma}_j^\alpha$ ($\alpha = x, y, z$) are the Pauli matrices for the jth site, $\langle j, l\rangle$ denotes the nearest-neighbor interactions, and J_α is the coupling strength. In addition, we assume that each spin couples with a Markovian bath individually, which tends to incoherently flip the spin down to the z direction. Under the Born-Markovian approximation and the secular approximation, the dissipator in Eq. (1) is given by

$$\sum_j \mathcal{D}_j[\hat{\rho}] = \frac{\gamma}{2}\sum_j[2\hat{\sigma}_j^-\hat{\rho}\hat{\sigma}_j^+ - \{\hat{\sigma}_j^+\hat{\sigma}_j^-, \hat{\rho}\}], \tag{12}$$

where $\hat{\sigma}_j^\pm = (\hat{\sigma}_j^x \pm i\hat{\sigma}_j^y)/2$ are the raising and lowering operators, respectively, γ is the decay rate, and $\{\cdot,\cdot\}$ denotes the anticommutator. The master equation admits a $\mathbb{Z}_2$ symmetry, which means that the system is invariant after a π rotation of all spins along the z axis ($\hat{\sigma}_j^x \to -\hat{\sigma}_j^x, \hat{\sigma}_j^y \to -\hat{\sigma}_j^y \forall j$). Hereinafter we set $\gamma = 1$.

Generally, in the thermodynamic limit, all the spins in steady states will point down along the z axis with zero magnetization on the xy plane, which is referred to as the paramagnetic (PM) phase. However, as the coupling strength varies, the steady states of the system may undergo a phase transition to the ordered phase with nonzero magnetization on the xy plane, which is referred to as the ferromagnetic (FM) phase, implying the spontaneous breaking of $\mathbb{Z}_2$ symmetry. The steady-state phase transitions in the dissipative spin-1/2 XYZ model has been widely studied throughout the literature [8,9,14,15,26,28].

Here we briefly review the steady-state properties of the model considered. By means of Gutzwiller mean-field factorization, the density matrix for the total system can be factorized as the tensor product of the density matrices of each site, $\hat{\rho} = \bigotimes_j \hat{\rho}_j$. All sites are assumed to be identical. As a consequence, Eq. (1) is reduced to a single-site master equation for a single-qubit system as

$$\frac{d\hat{\rho}}{dt} = -i[\hat{H}^{\rm MF}, \hat{\rho}] + \frac{\gamma}{2}[2\hat{\sigma}^-\hat{\rho}\hat{\sigma}^+ - \{\hat{\sigma}^+\hat{\sigma}^-, \hat{\rho}\}], \tag{13}$$

where the mean-field Hamiltonian $\hat{H}^{\rm MF}$ is given by

$$\hat{H}^{\rm MF} = \sum_{\alpha=x,y,z} J_\alpha\langle\hat{\sigma}^\alpha\rangle\hat{\sigma}^\alpha, \tag{14}$$

with $\langle\hat{\sigma}^\alpha\rangle = \mathrm{Tr}(\hat{\sigma}^\alpha\hat{\rho})$. By performing the integral on Eq. (13), the self-consistent master equation will finally converge to an asymptotic steady state. It is easy to find the paramagnetic state with all the spins pointing down in the z direction, $\hat{\rho}_\downarrow = \bigotimes_j \hat{\rho}_{j,\downarrow}$, where $\hat{\rho}_{j,\downarrow} = |\downarrow_j\rangle\langle\downarrow_j|$ is always a steady-state solution to Eq. (13).

Now we check the linear stability of the paramagnetic steady-state solution to the fluctuations [48–51]. The fluctuations are added to each site as follows:

$$\hat{\rho} = \bigotimes_j(\hat{\rho}_j + \delta\rho_j). \tag{15}$$

By performing the Fourier transform on the fluctuations $\delta\rho_j^{\mathbf{k}} = \sum_{\mathbf{k}} e^{-i\mathbf{k}\cdot\mathbf{r}_j}\delta\rho_j$ and substituting the perturbed density matrix in Eq. (15), we can decouple the master equation (13) in the momentum space as $\partial_t\delta\rho^{\mathbf{k}} = \mathcal{L}_{\mathbf{k}}\cdot\delta\rho^{\mathbf{k}}$. The

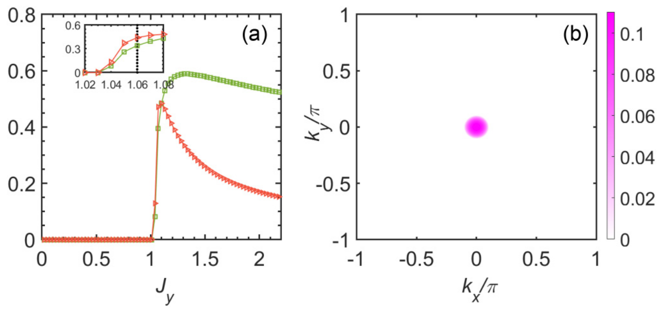

FIG. 1. (a) Mean-field steady-state magnetizations for $\langle\hat{\sigma}^x\rangle_{\rm SS}$ (squares) and $\langle\hat{\sigma}^y\rangle_{\rm SS}$ (triangles) as a function of J_y. (b) Real part of the most unstable eigenvalue of the superoperator $\mathcal{L}_{\mathbf{k}}$ in Eq. (16) as a function of k_x and k_y for $J_y = 1.06$. The other parameters are $J_x = 0.9$ and $J_z = 1$.

superoperator $\mathcal{L}_{\mathbf{k}}$ reads

$$\mathcal{L}_{\mathbf{k}} = \begin{pmatrix} -\gamma & 0 & 0 & 0 \\ 0 & P-\frac{\gamma}{2} & Q & 0 \\ 0 & -Q & -P-\frac{\gamma}{2} & 0 \\ \gamma & 0 & 0 & 0 \end{pmatrix}, \tag{16}$$

where the coefficients are $P = -i[(J_x + J_y)t_{\mathbf{k}} - 2\mathfrak{z}J_z]$ and $Q = -i(J_x - J_y)t_{\mathbf{k}}$, $\mathfrak{z} = 4$ is the coordination number of two-dimensional square lattice, the vector is given by $t_{\mathbf{k}} = 2\cos(k_x a) + 2\cos(k_y a)$, and a is the lattice constant. The stability of the paramagnetic steady state can be revealed by the eigenvalue spectrum of the superoperator $\mathcal{L}_{\mathbf{k}}$. If the real parts of all the eigenvalues of $\mathcal{L}_{\mathbf{k}}$ are negative, the system is stable under perturbation; otherwise, the system is unstable. Meanwhile, the critical points of the PM-FM phase transition can be analytically determined by the eigenvalues of the Jacobian. The Jacobian is obtained by the system of nonlinear Bloch equations [8,51]. The phase boundary can be expressed as

$$J^c_{x,y} = \frac{1}{16\mathfrak{z}^2}\frac{1}{J_z - J_{y,x}} + J_z. \tag{17}$$

In Fig. 1(a) we show the steady-state magnetizations in the xy plane as a function of J_y. One can find that for $J_y < J_y^{(c)} \approx 1.0391$, the steady-state magnetizations are $\langle\sigma^x\rangle_{\rm SS} = \langle\sigma^y\rangle_{\rm SS} = 0$. When J_y goes across the critical point $J_y^{(c)}$, the magnetizations in the xy plane become nonzero, indicating the appearance of a continuous phase transition from the disordered PM phase to the ordered FM phase with $\mathbb{Z}_2$ symmetry breaking. In particular, for $J_y > J_y^{(c)}$, the state $\hat{\rho}_\downarrow$ is unstable to the uniform spatial perturbations, as shown in Fig. 1(b). One can see that the system is mostly unstable to the perturbations with wave vector $\mathbf{k} = (0, 0)$ and will be eventually driven to the FM phase. For the case of $J_x = 0.9$ and $J_z = 1$, under the mean-field approximation, the critical point can be analytically determined by Eq. (17).

Now we investigate the susceptibilities of fidelity and trace distance in the vicinity of the phase transition by varying the coupling strength. The amount of variation δJ_y should be sufficiently small by definition. In Fig. 2 we check the convergence of the fidelity susceptibility, which is computed with various magnitudes of δJ_y. It is shown that the fidelity susceptibility starts to converge at $\delta J_y = 10^{-3}$. In the rest of the discussion of this model, unless stated otherwise, the parameter perturbation is fixed at $\delta J_y = 10^{-3}$.

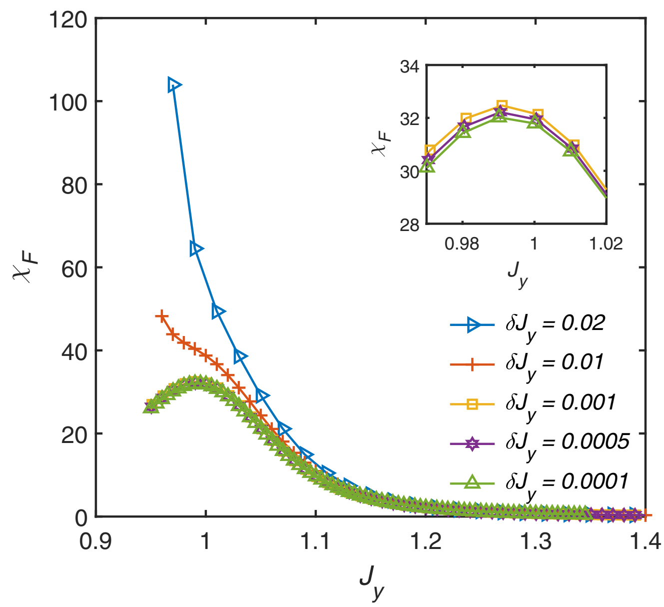

FIG. 2. In different scales of perturbations δJ_y, the fidelity susceptibility χ_F as a function of J_y for a 2×2 square lattice. The parameters are $J_x = 0.9$ and $J_z = 1$. The inset shows a close-up of the curves corresponding to $\delta J_y \leqslant 10^{-3}$.

With the periodic boundary condition, the steady states are obtained as follows: For the 2×2 and 2×3 lattices, we exactly diagonalize the Liouvillian superoperator $\mathcal{L}$ and take the eigenstate associated with the zero eigenvalue as the steady state, while for the 3×3 and 3×4 lattices, we numerically integrate the master equation via the fourth-order Runge-Kutta method and obtain the steady states by looking at the density matrix in the long-time limit, i.e., $\hat{\rho}_{\rm SS} = \lim_{t\to+\infty} e^{\mathcal{L}t}\hat{\rho}(0)$.

In Fig. 3 we show the fidelity susceptibility χ_F as a function of the coupling strength J_y for the lattices of different sizes. One can see that the maximum of χ_F always appears in the vicinity of $J_y = 1$, indicating the abrupt change for the steady-state density matrices. Moreover, the peak of χ_F becomes sharper as the size of the lattice increases. The inset of Fig. 3 shows the scaling of the maximum fidelity susceptibility versus the lattice size. We find the power-law dependence of the maxima on the size of lattice as

$$\chi_F^{\rm max} \sim \kappa L^\eta, \tag{18}$$

where $L = N^{1/d}$ is the linear dimension of the system, $d = 2$ is the real dimension, and N is the number of sites. Then we obtain the corresponding fitting parameters $\eta \approx 1.7572$ and $\kappa \approx 2.2162$.

Now we discuss our results within the scope of the scaling hypothesis. Suppose that, near the critical point J_y^c, the average fidelity susceptibility $\chi_F(J_y, L)/L^d$ of a cluster of size $N = L^d$ scales as

$$\frac{\chi_F(J_y, L)}{L^d} \sim \frac{1}{|J_y - J_y^c|^\alpha}, \tag{19}$$

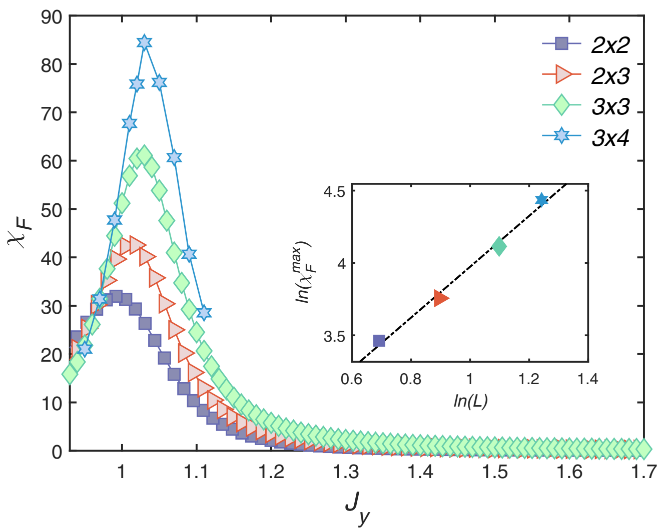

FIG. 3. Fidelity susceptibility χ_F as a function of J_y for 2×2, 2×3, 3×3, and 3×4 lattices, with fixed $J_x = 0.9$ and $J_z = 1$. The inset shows the maximum of the fidelity susceptibility $\chi_F^{\max}$ versus the linear dimension L (log-log scale) with a power-law fitting (dash-dotted line).

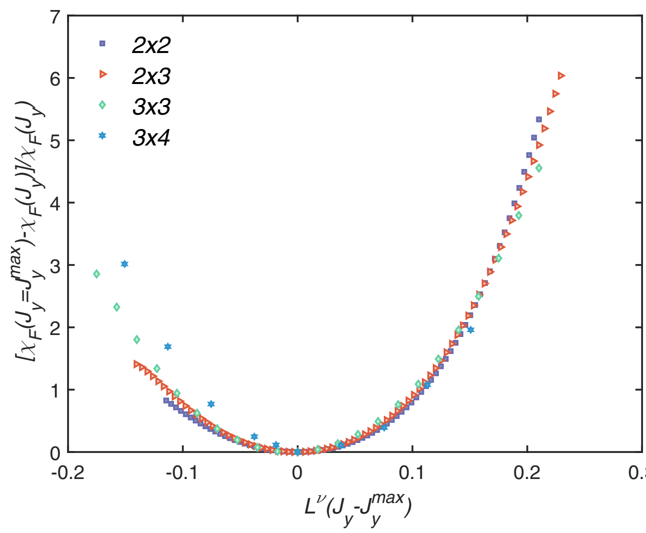

FIG. 4. Rescaled fidelity susceptibility as a function of $L^\nu(J_y - J_y(\chi_F^{\max}))$ in the finite-size scaling analysis of the two-dimensional dissipative XYZ model. The critical exponent for the correlation length is estimated to be $\nu = 0.48 \pm 0.06$. The parameters are $J_x = 0.9$ and $J_z = 1$.

where α is the corresponding exponent. Inspired by the proposals by Gu *et al.* [33] and taking into account Eq. (18), the rescaled fidelity susceptibility as a function of the rescaled coupling strength is given by

$$\frac{\chi_F\big(J_y\big(\chi_F^{\max}\big), L\big) - \chi_F(J_y, L)}{\chi_F(J_y, L)} = f\big[L^\nu\big(J_y - J_y\big(\chi_F^{\max}\big)\big)\big], \quad (20)$$

where ν is the critical exponent of correlation length. In deriving Eq. (20), we have rewritten Eq. (18) as $\chi_F(J_y(\chi_F^{\max}), L) \sim L^\eta$, in which $J_y(\chi_F^{\max})$ is the coupling strength for the maximal fidelity susceptibility in lattices of different sizes. Consequently, we have the relationship

$$\nu = \frac{\eta - d}{\alpha}. \quad (21)$$

In Fig. 4 we show the rescaled fidelity susceptibilities with respect to the rescaled coupling strength. One can see that the data collapse with the estimated critical exponent $\nu = 0.48 \pm 0.06$. Unfortunately, a direct estimation of the critical exponent ν in the dissipative quantum XYZ model is not available and so we could not benchmark our estimation of ν. Note that the estimation is based on relatively small lattices, so the result should be interpreted with caution.

In order to estimate the critical point J_y^c of the phase transition, we linearly fit the critical coupling strengths $J_y(\chi_F^{\max})$, which correspond to the extreme points of χ_F, to the system size N. As shown in Fig. 5, with increasing system size, the critical coupling strength $J_y(\chi_F^{\max})$ converges. In the thermodynamic limit, i.e., $1/N \to 0$, the critical coupling strength can be estimated as $J_y^c \approx 1.05$. For comparison, in the cluster mean-field and Gutzwiller Monte Carlo calculations the critical points are estimated to be $J_y^c \approx 1.04$ [8,52], by means of the quantum trajectory method the critical point is estimated to be $J_y^c \approx 1.04$ [28], and the corner-space renormalization predicts a phase transition at $J_y^c \approx 1.07$ [26].

In Fig. 6 we show the trace distance susceptibility as a function of J_y. One can see that, as the lattice size N increases the χ_T shows a critical behavior which is similar to the fidelity susceptibility. Near the critical point of the PM-FM phase transition, the maximal value of χ_T keeps growing as the size increases. Although the peak values are not growing as fast as the results of the fidelity susceptibility, a power-law fit for the peaks of the χ_T and the lattice number still can be found, $\chi_T^{\max} \propto L^\zeta$ with $\zeta \approx 0.8921$. By linearly fitting the $J_y^{\max}(N)$ to the system size N, we obtain the critical point in the thermodynamic limit as $J_y^c \approx 1.05$. This result is in good agreement with the existing results [8,26,28,52].

B. Driven-dissipative Kerr model

In this section we concentrate on a driven-dissipative Kerr model as an example of a second-order dissipative phase

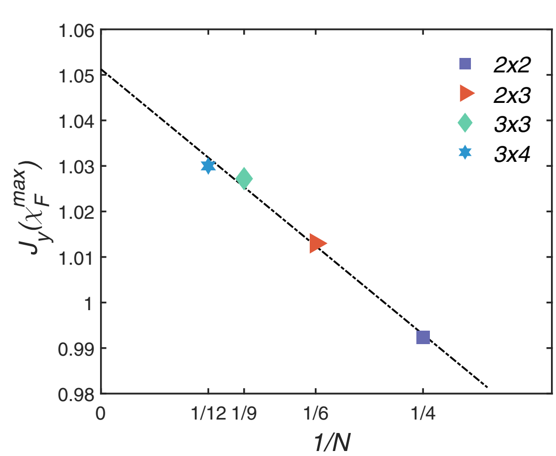

FIG. 5. Coupling strengths corresponding to the maximum $\chi_F^{\max}$ as a function of the different system sizes $1/N$. The dash-dotted line is the linear fitting. The other parameters are $J_x = 0.9$ and $J_z = 1$.

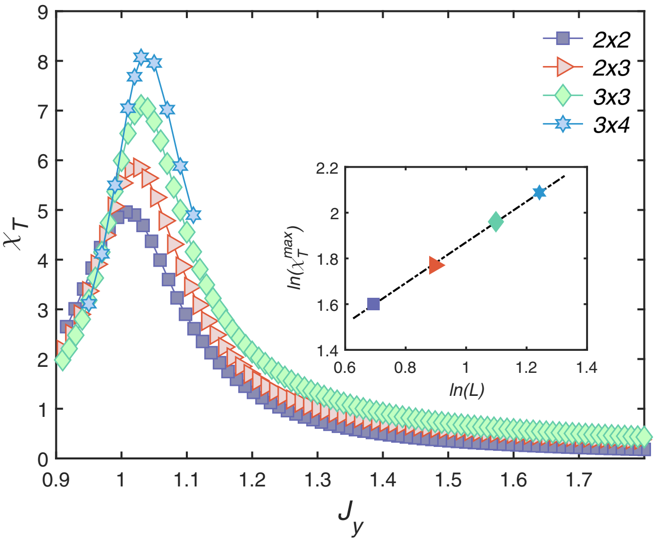

FIG. 6. Trace distance susceptibility versus the coupling parameter J_y for 2×2, 2×3, 3×3, and 3×4 lattices. The inset shows the maximum of the trace distance susceptibility $\chi_T^{\max}$ versus the linear dimension L (log-log scale) with a power-law fitting (dash-dotted line). The other parameters are $J_x = 0.9$, $J_z = 1$, and $\delta J_y = 0.0001$.

transition with symmetry breaking in the continuous variable (CV) system. The specific model we investigate is a typical nonlinear oscillator with two-photon pumping but single-photon dissipation. This model has already been studied in Ref. [53], where the authors investigated the properties of the continuous phase transition by means of mean-field theory, exact diagonalization, and the Keldysh formalism.

Here we briefly review the previous work studied by Zhang and Baranger [53]. In a rotating frame, the considered Hamiltonian can be obtained as

$$\hat{H} = -\Delta \hat{a}^\dagger \hat{a} + \frac{U}{2}\hat{a}^\dagger \hat{a}^\dagger \hat{a}\hat{a} + \frac{G}{4}(\hat{a}^\dagger \hat{a}^\dagger + \hat{a}\hat{a}), \tag{22}$$

where $\Delta = \omega_p - \omega_c$ is the detuning of the frequency of pumping ω_p and cavity ω_c, U quantifies the Kerr nonlinearity, and G is the amplitude of the two-photon driving. The specific single-photon dissipation is described by

$$\mathcal{D}[\hat{\rho}] = \frac{\gamma}{2}(2\hat{a}\hat{\rho}\hat{a}^\dagger - \{\hat{a}^\dagger \hat{a}, \hat{\rho}\}), \tag{23}$$

where γ is the decay rate. Again we will work in units of γ. Substituting the Hamiltonian (22) and the dissipator (23) into Eq. (1), we can find a discrete $\mathbb{Z}_2$ symmetry associated with the master equation. The corresponding symmetry superoperator is given by

$$\mathcal{Z}_2 \bullet = e^{i\pi \hat{a}^\dagger \hat{a}} \bullet e^{-i\pi \hat{a}^\dagger \hat{a}}, \tag{24}$$

where the symbol $\bullet$ denotes the steady-state density matrix.

Under the semiclassical approximation, in which all the quantum fluctuations and quantum correlations become negligible, i.e., $\langle \hat{a}^\dagger \hat{a}\hat{a}\rangle \approx \langle \hat{a}^\dagger\rangle\langle \hat{a}\rangle\langle \hat{a}\rangle$, we can obtain the equation of motion for the coherent field amplitude $\alpha = \langle \hat{a}\rangle$ in the resonant case ($\Delta = 0$) [54]

$$\frac{d}{dt}\alpha = \left(-iU|\alpha|^2 - \frac{\gamma}{2}\right)\alpha - i\frac{G}{2}\alpha^*. \tag{25}$$

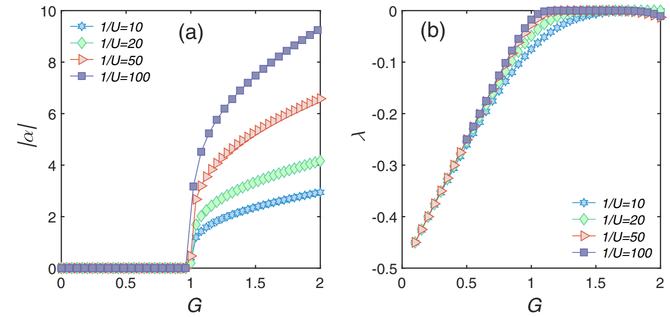

FIG. 7. (a) Modulus of the steady-state coherent field amplitude $|\alpha|$ versus the two-photon driving G under the semiclassical approximation treatment for the different Kerr nonlinearities. (b) Liouvillian gap $\lambda = \mathrm{Re}[\lambda_1]$ as a function of the two-photon driving strength G with the different Kerr nonlinearity.

The steady-state value of α can be obtained by numerically evolving the self-consistent equation of motion (25) for a sufficiently long time. The steady-state value of $|\alpha_{SS}|$ is considered as the order parameter. Namely, a zero $|\alpha_{SS}|$ indicates the disordered phase, while a nonzero $|\alpha_{SS}|$ indicates the ordered phase with $\mathbb{Z}_2$ symmetry breaking. By analyzing the semiclassical equation (25), the number of photons n in the cavity is of order γ/U and the thermodynamic limit can be achieved in the limit of infinitesimal interaction $U/\gamma \to 0^+$ [53].

Figure 7(a) shows the modulus of the steady-state coherent field amplitude as a function of the two-photon driving strength G. For different values of the Kerr nonlinearity strength, the order parameter $|\alpha|$ always shows a transition from the zero value to a finite constant, implying the emergence of a second-order phase transition. At the level of the semiclassical approximation, the critical point of this dissipative quantum phase transition is near $G_c \approx 1$.

Now we go beyond the semiclassical approximation and concentrate on the quantum level. We show the Liouvillian gap $\lambda = \mathrm{Re}[\lambda_1]$ in Fig. 7(b). One can see that with decreasing Kerr nonlinearity, the Liouvillian gap tends to zero faster. For the minimum Kerr nonlinearity strength $U = 1/100$, the Liouvillian gap closes in the interval of $G \in (1, 2)$. This implies that the two degenerate steady states break the $\mathbb{Z}_2$ symmetry spontaneously, characterizing the occurrence of the second-order phase transition [41].

In Fig. 8 we show that the numerics of the fidelity susceptibility χ_F changes with the two-photon driving G. The different markers label the results of the corresponding Kerr nonlinearity strengths U. Analogous to the spin model discussed in Sec. III A, the abrupt changes for the steady-state density matrices contribute to the peak patterns. As the number of photons increases, the maximum of $\chi_F^{\max}$ remains higher and the peak gets sharper. Moreover, with decreasing nonlinearity U to the thermodynamic limit, the critical two-photon driving $G(\chi_F^{\max})$ shifts towards the left. In the inset of Fig. 8, we report the scaling of $G(\chi_F^{\max})$ with the Kerr nonlinearity U. Through the linear fitting, one can approximately estimate the critical value as $G^c \approx 1.04$.

The divergence can also be observed in the behavior of trace distance susceptibility χ_T as shown in Fig. 9. Following

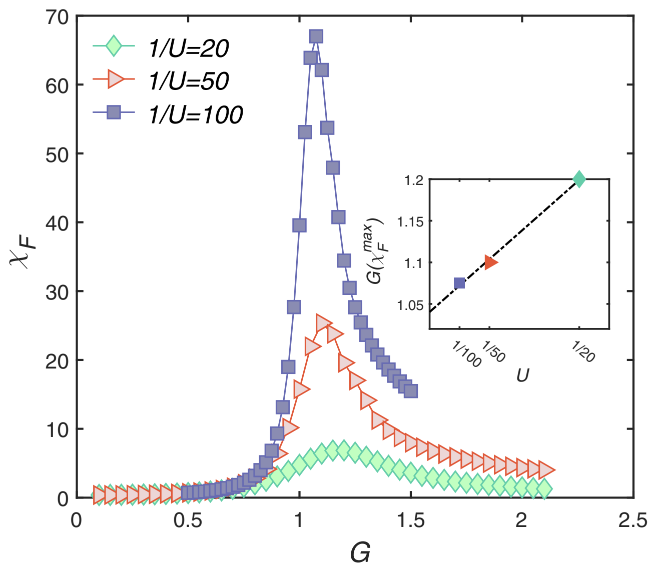

FIG. 8. Fidelity susceptibility χ_F of the single Kerr oscillator versus the two-photon driving strength G. The different markers indicate that the results are simulated with different numbers of photons in the cavity. The inset shows the critical two-photon driving $G(\chi_F^{\max})$ versus Kerr nonlinearity U; the dash-dotted line indicates the finite-size linear fitting.

the same analysis routine for χ_F, we find that χ_T becomes divergent as the two-photon driving strength G approaches the critical point. As the Kerr nonlinearity U decreasing, the divergent behavior of χ_T becomes more and more apparent, i.e., the heights of the peaks become higher and the positions critical values of two-photon driving $G(\chi_\mathrm{T}^{\max})$ shift

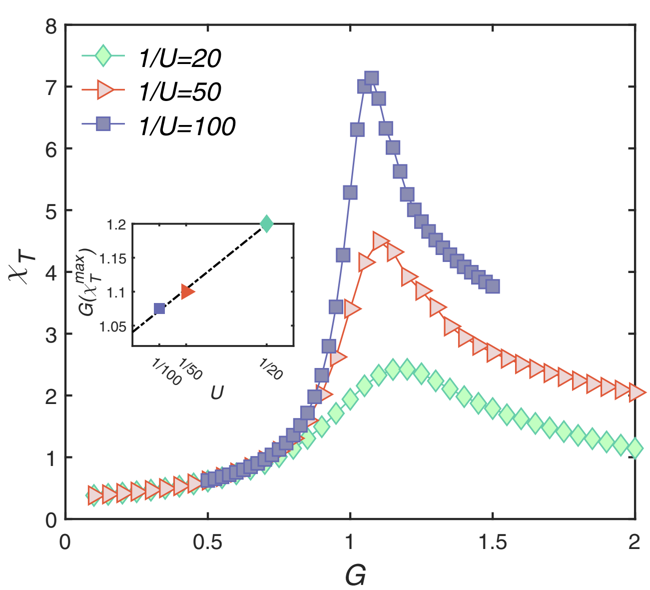

FIG. 9. Trace distance susceptibility χ_T of the single Kerr oscillator versus the two-photon driving strength G. The different markers indicate that the results are simulated with different numbers of photons in the cavity. The inset shows the critical two-photon driving $G(\chi_T^{\max})$ versus Kerr nonlinearity U; the dash-dotted line indicates the finite-size linear fitting.

to the left. The linear fitting of $G(\chi_T^{\max})$ to the nonlinearity allow us to extrapolate the critical value of two-photon driving to be $G^c \approx 1.04$, consistent with the results obtained by the fidelity susceptibility.

IV. SUMMARY

We have utilized the susceptibilities of the fidelity and trace distance to detect steady-state phase transitions in dissipative quantum systems. Different from previous studies of dissipative phase transitions based on appropriately chosen order parameters, the two indicators proposed in this paper are observable independent and, more interestingly, are direct reflections of the abrupt changes of similarities between the steady states when the system undergoes a phase transition.

As applications we mainly investigated the dissipative spin-1/2 XYZ model on a two-dimensional square lattice and a driven-dissipative Kerr oscillator. It has been shown that both models may undergo continuous steady-state phase transitions (breaking $\mathbb{Z}_2$ symmetry) via tuning the controlling parameters.

In the former model, we first confirmed the existence of a continuous phase by means of the mean-field approximation and the linear stability analysis. Then we studied the behaviors of the fidelity susceptibility and trace distance susceptibility of steady states as functions of coupling strength. We found the divergent behaviors of the susceptibilities near the phase transitions which stem from the abrupt change of the state similarity between two steady states when the systems undergo the phase transition. We performed finite-size scaling analysis on the fidelity susceptibility. Within the scope of the scaling hypothesis, we estimated the values of the corresponding critical exponents. Moreover, the finite-size scaling of the critical coupling strength and the system size enabled us to estimate the true critical point in the thermodynamic limit. In the latter CV model, we revisited the steady-state properties obtained by the semiclassical treatment. Analogous to the spin model, the singular behaviors of susceptibilities as functions of the two-photon driving strength were observed, which indicates the occurrence of dissipative phase transitions. In particular, the scaling of the critical driving strength to the Kerr nonlinearity allowed us to extrapolate the critical point in the thermodynamic limit ($U \to 0$). The critical points in thermodynamic limit, accessed from the analysis on the fidelity and trace distance susceptibilities, agree well with the existing results obtained by other methods.

Finally, the investigation of the dissipative quantum phase transition is still a hard task, especially for quantum many-body systems. The exponential growth of the quantum many-body Hilbert space restricts the ability to directly witness the phenomenon of phase transitions. Fortunately, the critical behaviors of the fidelity susceptibility, trace distance susceptibility, angularly averaged magnetic susceptibility, and quantum Fisher information can indirectly reveal the existence of the phase transitions. Along these lines, the combination of the fidelity susceptibility and trace distance susceptibility with other state-of-the-art simulation strategies for exploring larger lattices is promising, such as the matrix-product-operator approach [55] and neural networks

[56–60]. Future exploration of other physical models and phenomena, e.g., geometrical frustration [51,61–63], is also an intriguing perspective.

ACKNOWLEDGMENTS

This work was supported by the National Natural Science Foundation of China via Grant No. 11975064.

[1] S. Sachdev, *Quantum Phase Transitions* (Cambridge University Press, Cambridge, 2000).
[2] L. Amico, R. Fazio, A. Osterloh, and V. Vedral, Rev. Mod. Phys. **80**, 517 (2008).
[3] G. Lindblad, On the generators of quantum dynamical semigroups, Commun. Math. Phys. **48**, 119 (1976).
[4] V. Gorini, A. Kossakowski, and E. C. Sudarsahan, Completely positive dynamical semigroups of N-level systems, J. Math. Phys. **17**, 821 (1976).
[5] H.-P. Breuer and F. Peturccione, *The Theory of Open Quantum Systems* (Oxford University Press, New York, 2002).
[6] M. Henkel, H. Hinrichsen, and S. Lübeck, *Non-Equilibrium Phase Transitions* (Springer, Berlin, 2008), Vol. 1.
[7] M. Henkel and M. Pleimling, *Non-Equilibrium Phase Transitions* (Springer, Berlin, 2010), Vol. 2.
[8] J. Jin, A. Biella, O. Viyuela, L. Mazza, J. Keeling, R. Fazio, and D. Rossini, Cluster Mean-Field Approach to the Steady-State Phase Diagram of Dissipative Spin Systems, Phys. Rev. X **6**, 031011 (2016).
[9] A. Biella, J. Jin, O. Viyuela, C. Ciuti, R. Fazio, and D. Rossini, Linked cluster expansions for open quantum systems on a lattice, Phys. Rev. B **97**, 035103 (2018).
[10] R. Rota, F. Minganti, C. Ciuti, and V. Savona, Quantum Critical Regime in a Quadratically Driven Nonlinear Photonic Lattice, Phys. Rev. Lett. **122**, 110405 (2019).
[11] M. F. Maghrebi and A. V. Gorshkov, Nonequilibrium many-body steady states via Keldysh formalism, Phys. Rev. B **93**, 014307 (2016).
[12] V. R. Overbeck, M. F. Maghrebi, A. V. Gorshkov, and H. Weimer, Multicritical behavior in dissipative Ising models, Phys. Rev. A **95**, 042133 (2017).
[13] D. Huybrechts, F. Minganti, F. Nori, M. Wouters, and N. Shammah, Validity of mean-field theory in a dissipative critical system: Liouvillian gap, $\mathbb{PT}$-symmetric antigap, and permutational symmetry in the XYZ model, Phys. Rev. B **101**, 214302 (2020).
[14] D. Kilda, A. Biella, M. Schiró, R. Fazio, and J. Keeling, On the stability of the infinite projected entangled pair operator ansatz for driven-dissipative 2D lattices, SciPost Phys. Core **4**, 005 (2021).
[15] T. E. Lee, S. Gopalakrishnan, and M. D. Lukin, Unconventional Magnetism via Optical Pumping of Interacting Spin Systems, Phys. Rev. Lett. **110**, 257204 (2013).
[16] T. E. Lee, H. Hüffner, and M. C. Cross, Antiferromagnetic phase transition in a nonequilibrium lattice of Rydberg atoms, Phys. Rev. A **84**, 031402(R) (2011).
[17] M. Rigol, T. Bryant, and R. R. P. Singh, Numerical Linked-Cluster Approach to Quantum Lattice Models, Phys. Rev. Lett. **97**, 187202 (2006).
[18] B. Tang, E. Khatami, and M. Rigol, A short introduction to numerical linked-cluster expansions, Comput. Phys. Commun. **184**, 557 (2013).
[19] S. Finazzi, A. Le Boité, F. Storme, A. Baksic, and C. Ciuti, Corner-Space Renormalization Method for Driven-Dissipative Two-Dimensional Correlated Systems, Phys. Rev. Lett. **115**, 080604 (2015).
[20] H. Weimer, Variational Principle for Steady States of Dissipative Quantum Many-Body Systems, Phys. Rev. Lett. **114**, 040402 (2015).
[21] A. Kshetrimayum, H. Weimer, and R. Orús, A simple tensor network algorithm for two-dimensional steady states, Nat. Commun. **8**, 1291 (2017).
[22] C. Mc Keever and M. H. Szymańska, Stable iPEPO Tensor-Network Algorithm for Dynamics of Two-Dimensional Open Quantum Lattice Models, Phys. Rev. X **11**, 021035 (2021).
[23] J. Huber, P. Kirton, and P. Rabl, Phase-space methods for simulating the dissipative many-body dynamics of collective spin systems, SciPost Phys. **10**, 045 (2021).
[24] V. P. Singh and H. Weimer, Driven-dissipative criticality within the discrete truncated Wigner approximation, arXiv:2108.07273.
[25] J. Dalibard, Y. Castin, and K. Mølmer, Wave-Function Approach to Dissipative Processes in Quantum Optics, Phys. Rev. Lett. **68**, 580 (1992).
[26] R. Rota, F. Storme, N. Bartolo, R. Fazio, and C. Ciuti, Critical behavior of dissipative two-dimensional spin lattices, Phys. Rev. B **95**, 134431 (2017).
[27] F. Vicentini, F. Minganti, R. Rota, G. Orso, and C. Ciuti, Critical slowing down in driven-dissipative Bose-Hubbard lattices, Phys. Rev. A **97**, 013853 (2018).
[28] R. Rota, F. Minganti, A. Biella, and C. Ciuti, Dynamical properties of dissipative XYZ Heisenberg lattices, New J. Phys. **20**, 045003 (2018).
[29] S.-J. Gu, Fidelity approach to quantum phase transitions, Int. J. Mod. Phys. B **24**, 4371 (2010).
[30] P. Zanardi and N. Paunković, Ground state overlap and quantum phase transitions, Phys. Rev. E **74**, 031123 (2006).
[31] N. S. Tonchev, Mixed-state fidelity susceptibility through iterated commutator series expansion, Phys. Rev. E **90**, 052103 (2014).
[32] W.-L. You, Y.-W. Li, and S.-J. Gu, Fidelity, dynamic structure factor, and susceptibility in critical phenomena, Phys. Rev. E **76**, 022101 (2007).
[33] S.-J. Gu, H.-M. Kwok, W.-Q. Ning, and H.-Q. Lin, Fidelity susceptibility, scaling, and universality in quantum critical phenomena, Phys. Rev. B **77**, 245109 (2008).
[34] H.-M. Kwok, W.-Q. Ning, S.-J. Gu, and H.-Q. Lin, Quantum criticality of the Lipkin-Meshkov-Glick model in terms of fidelity susceptibility, Phys. Rev. E **78**, 032103 (2008).
[35] A. F. Albuquerque, F. Alet, C. Sire, and S. Capponi, Quantum critical scaling of fidelity susceptibility, Phys. Rev. B **81**, 064418 (2010).
[36] D. Rossini and E. Vicari, Ground-state fidelity at first-order quantum transitions, Phys. Rev. E **98**, 062137 (2018).

[37] L. Wang, Y.-H. Liu, J. Imriška, P. N. Ma, and M. Troyer, Fidelity Susceptibility Made Simple: A Unified Quantum Monte Carlo Approach, Phys. Rev. X **5**, 031007 (2015).
[38] S. Yang, S.-J. Gu, C.-P. Sun, and H.-Q. Lin, Fidelity susceptibility and long-range correlation in the Kitaev honeycomb model, Phys. Rev. A **78**, 012304 (2008).
[39] J. H. Zhao and H. Q. Zhou, Singularities in ground state fidelity and quantum phase transitions for the Kitaev model, Phys. Rev. B **80**, 014403 (2009).
[40] E. M. Kessler, G. Giedke, A. Imamoglu, S. F. Yelin, M. D. Lukin, and J. I. Cirac, Dissipative phase transition in a central spin system, Phys. Rev. A **86**, 012116 (2012).
[41] F. Minganti, A. Biella, N. Bartolo, and C. Ciuti, Spectral theory of Liouvillians for dissipative phase transitions, Phys. Rev. A **98**, 042118 (2018).
[42] A. Peres, Stability of quantum motion in chaotic and regular systems, Phys. Rev. A **30**, 1610 (1984).
[43] K. Życzkowski and H.-J. Sommers, Average fidelity between random quantum states, Phys. Rev. A **71**, 032313 (2005).
[44] A. Uhlmann, The "transition probability" in the state space of a *-algebra, Rep. Math. Phys. **9**, 273 (1976).
[45] H.-J. Sommers and K. Życzkowski, Bures volume of the set of mixed quantum states, J. Phys. A: Math. Gen. **36**, 10083 (2003).
[46] D. Šafránek, Discontinuities of the quantum Fisher information and the Bures metric, Phys. Rev. A **95**, 052320 (2017).
[47] M. M. Wilde, Quantum information theory lecture notes, http://www.markwilde.com/teaching/2015-fall-qit/lectures/lecture-14.pdf (2015).
[48] M. C. Cross and P. C. Hohenberg, Pattern formation outside of equilibrium, Rev. Mod. Phys. **65**, 851 (1993).
[49] A. Le Boité, G. Orso, and C. Ciuti, Steady-State Phases and Tunneling-Induced Instabilities in the Driven Dissipative Bose-Hubbard Model, Phys. Rev. Lett. **110**, 233601 (2013).
[50] A. Le Boité, G. Orso, and C. Ciuti, Bose-Hubbard model: Relation between driven-dissipative steady states and equilibrium quantum phases, Phys. Rev. A **90**, 063821 (2014).
[51] X. Li, J. Jin, Nonuniform phases in the geometrically frustrated dissipative XYZ model, Phys. Rev. B **103**, 035127 (2021).
[52] W. Casteels, R. M. Wilson, and M. Wouters, Gutzwiller Monte Carlo approach for a critical dissipative spin model, Phys. Rev. A **97**, 062107 (2018).
[53] X. H. H. Zhang and H. U. Baranger, Driven-dissipative phase transition in a Kerr oscillator: From semiclassical $\mathcal{PT}$ symmetry to quantum fluctuations, Phys. Rev. A **103**, 033711 (2021).
[54] I. Carusotto and C. Ciuti, Quantum fluids of light, Rev. Mod. Phys. **85**, 299 (2013).
[55] E. Mascarenhas, H. Flayac, and V. Savona, Matrix-product-operator approach to the nonequilibrium steady state of driven-dissipative quantum arrays, Phys. Rev. A **92**, 022116 (2015).
[56] M. J. Hartmann and G. Carleo, Neural-Network Approach to Dissipative Quantum Many-Body Dynamics, Phys. Rev. Lett. **122**, 250502 (2019).
[57] A. Nagy and V. Savona, Variational Quantum Monte Carlo Method with a Neural-Network Ansatz for Open Quantum Systems, Phys. Rev. Lett. **122**, 250501 (2019).
[58] F. Vicentini, A. Biella, N. Regnault, and C. Ciuti, Variational Neural-Network Ansatz for Steady States in Open Quantum Systems, Phys. Rev. Lett. **122**, 250503 (2019).
[59] N. Yoshioka and R. Hamazaki, Constructing neural stationary states for open quantum many-body systems, Phys. Rev. B **99**, 214306 (2019).
[60] D. Yuan, H. Wang, Z. Wang, and D.-L. Deng, Solving the Liouvillian Gap with Artificial Neural Networks, Phys. Rev. Lett. **126**, 160401 (2021).
[61] X. Li, Y. Li, and J. Jin, Steady-state phases of dissipative spin-1/2 XYZ model with frustrated interaction, Phys. Rev. B **104**, 155130 (2021).
[62] J. Qian, L. Zhou, and W. Zhang, Quantum phases of strongly interacting Rydberg atoms in triangular lattices, Phys. Rev. A **87**, 063421 (2013).
[63] Z. Li, A. Soret, and C. Ciuti, Dissipation-induced antiferromagneticlike frustration in coupled photonic resonators, Phys. Rev. A **103**, 022616 (2021).